Journal of Magnetic Resonance **141,** 62–67 (1999)
Article ID jmre.1999.1874, available online at http://www.idealibrary.com on IDEAL®

Phase-Modulated Rotating-Frame NQR Techniques for Spatial Encoding

F. Casanova, H. Robert,[1] and D. Pusiol

Facultad de Matemática, Astronomía, y Física, Universidad Nacional de Córdoba, Ciudad Universitaria, 5000 Córdoba, Argentina

Received January 8, 1999; revised July 9, 1999

The rotating-frame method of localization for spatially resolved spectroscopy and imaging in the pure quadrupole regime relies on a gradient B_1 field in which spins experience a flip angle dependent on their position in the B_1 field strength. So far, the techniques have been implemented as amplitude-modulated methods, i.e., the spatial nuclear quadrupole distribution is encoded in the amplitude of the free-induction decay signals. In this work, we describe the implementation of phase-modulated variants of both two-dimensional and rapid rotating-frame imaging techniques. The experiments are discussed for both single crystalline and powder samples. The phase-modulated experiment offers some advantages over the amplitude-encoding technique: It enables one to distinguish the sign of the spatial coordinate and the signal-to-noise ratio is higher than for the simplest amplitude-encoding method.

Key Words: **nuclear quadrupole resonance; spatially resolved NQR spectroscopy; NQR imaging.**

INTRODUCTION

In rotating-frame NQR (ρNQR) localized spectroscopy (*1–3*) and imaging (*4, 5*), spatial information is encoded using radiofrequency field B_1 gradients. These encoding techniques are based on the principle that the effective B_1 field strength experienced by a nuclear spin depends on its position along the axis defined by the RF gradient.

The ρNQR experiments described in the literature rely on amplitude-modulated methods: In the two-dimensional variant of the technique (*1*), free-induction decay signals are measured as a function of the length of a square RF excitation pulse and the spatial information becomes encoded in the amplitude of the FID signals. For the single-experiment imaging technique (*4*), a train of small flip angle pulses is applied with a gradient so that the spatial distribution of spins modulates the amplitude of the magnetization stroboscopically acquired in the gaps between pulses.

As was suggested by Hoult in the original paper on NMR rotating-frame imaging (*6*), the amplitude-modulated experiment can be converted to a phase-modulated form if the incremental pulses applied for spatial encoding are immediately followed by a uniform 90° plane-rotation pulse that is 90° out of phase with the preceding pulse. Since the uniform 90° pulse will rotate all the magnetization vectors onto the transverse plane, the spatial information in the magnetization grid prepared by the first pulse is converted to a relative phase between the magnetization vector and the axis defined by the first B_1 field. Therefore, the spatial frequencies are sampled through the phase modulation of the spin magnetization varying the duration of the preparatory pulse. The maximum possible sensitivity in a rotating-frame experiment is achieved with the phase-encoding variant.

The application of a phase-modulated approach to NQR, however, has been hindered by the fact that the induced magnetization vector in a quadrupole system is always aligned in the direction of the B_1 field (*7*). The magnetization vector oscillates rather than precesses, so that one would not, at first sight, expect to be able to phase encode. Besides the well-known difficulties of using a classical picture for the description of a quadrupole system, there is also the problem of nonuniform magnetization rotations in a polycrystalline object due to the powder distribution of nutation frequencies. Because of these particularities of the spin dynamics in quadrupole systems, it is not obvious that phase modulation of the NQR signal can be used for spatial encoding.

Recently, we have demonstrated that a phase-modulated version of the nutation frequency technique is possible for NQR. The two-dimensional phase-modulated nutation frequency method (*8*) was applied to spin $I = 3/2$ system for the determination of the asymmetry parameter η in powder specimens. Theoretical analysis and experimental results show that the phase-modulated variant of nutation spectroscopy is feasible in the pure quadrupole regime and it provides a gain in the signal-to-noise ratio of the Fourier-transformed spectrum compared to the amplitude-modulated method.

In this paper, we study the application of phase-encoding variants of both two- and one-dimensional rotating-frame NQR techniques. The first goal is to demonstrate the feasibility of a two-dimensional phase-modulated method for spatial localization. The second aim is to develop a novel variant of the one-dimensional or rapid rotating-frame imaging technique that encodes spin position in the phase of the strobocopically

[1] Present address: Quantum Magnetics, 7740 Kenamar Court, San Diego, CA 92121.

1090-7807/99 $30.00

acquired system magnetization. It is shown that the phase-modulated variants of the rotating-frame NQR methods provide a gain in the signal-to-noise ratio, compared with the amplitude encoding versions, and enables one to resolve the sign of precession in the rotating frame, thus allowing an effective discrimination of positive and negative spatial coordinates. The implementations of these methods are advantageous because the higher sensitivity allows one to reduce data acquisition time, and the discrimination of positive and negative coordinates enables us to make use of the whole volume in some coil configuration, such as the reversed Helmholtz coil.

TWO-DIMENSIONAL PHASE-ENCODING TECHNIQUE

The composite pulse for 2D phase encoding consists of two 90° phase-shifted radiofrequency pulses with no delay within the sequence. The pulse sequence can be denoted

$$(G_1t_1)_0 - (B_2t_2)_{\pi/2} - acq,$$

where $(G_1t_1)_0$ is a variable pulse of length t_1 and zero phase applied with a gradient G_1 for spatial encoding, and it is followed by a homogeneous B_2 pulse of fixed duration t_2 that is 90° out of phase with the first one. The second pulse converts the amplitude modulation created by the first period of RF irradiation in phase modulation. The NQR signal is acquired during the interval of free evolution after the pulses.

The excitation fields B_i, $i = 1, 2$, are assumed to be parallel everywhere over the sample volume. Therefore, the effective flip angle induced by the RF field of amplitude B_i is $\alpha_i = \gamma\lambda(\theta, \phi)B_it_i$. For $I = 3/2$ the function

$$\lambda(\theta, \phi) = \frac{1}{2\sqrt{3 + \eta^2}}[(2\eta \cos \theta)^2 + \sin^2\theta(9 + \eta^2 + 6\eta \cos 2\phi)]^{1/2}$$

determines the effective RF field strength seen in the EFG principal axis system oriented θ and ϕ with respect to the B_i field.

The dependence of the magnetization as a function of the flip angles is obtained by direct calculation of the evolution of the spin system using the quadrupole interaction representation (QIR) formalism developed by Pratt (*9*). In the QIR formalism, a set of three operators $\{Y_x, Y_y, Y_z\}$ forms a complete basis for an ensamble of noninteracting quadrupole nuclei, and the commutation properties define a simple transformation relationship among these operators. Therefore, the dynamics of quadrupole spin-3/2 system are confined to a three dimensional space and allow one to describe in a straightforward way the evolution of the $I = 3/2$ quadrupole system during and after being excited by RF pulses. The quadrature-detected NQR signal is calculated as the expectation values of $\lambda(\theta, \phi)$ $(Y_x \cos \psi + Y_y \sin \psi)$ for the reference phases $\psi = 0$ and $\psi = 90°$. This formalism (*9, 10*) and several of its applications to the description of different pulse sequences have been published elsewhere (*4, 11–13*).

The operators Y_p $(p = x, y, z)$ depend on the geometrical parameters θ and ϕ; therefore, a particular basis set of operators can describe the spin dynamics of only one crystalline domain of the sample. To calculate the response for a powder specimen, the strategy is to calculate the response of a single crystal with an arbitrary orientation with respect to the RF field. Then, the total signal from the polycrystalline sample is obtained as a superposition of signals for all the possible orientations of the EFG's axes.

In a previous work, we calculated the response of an $I = 3/2$ quadrupole system to the pulse sequence $(B_1t_1)_0 - (B_1t_2)_{\pi/2} - acq$ for phase-modulated nutation frequency spectroscopy, where (B_1t_i) denotes a homogeneous pulse of length t_i. The calculations have been outlined in Ref. (*8*) and they can easily be modified for the application of the technique for spatial encoding, including the spatial dependence of the B_1 field in the corresponding flip angle. In the following, we merely summarize the results of the calculations and discuss the particulars of this technique for NQR imaging.

Response of a Single Crystal to the Pulse Sequence for Phase Encoding

We begin by considering the application of the technique to a single crystalline sample. In this case, there is no powder distribution of the effective nutation frequencies and there are well-defined magnetization rotations. Therefore, the spatial spin distribution in the object can directly be reconstructed by the Fourier transform and thus makes it possible to compare the spectral sensitivities obtained by the amplitude- and phase-modulated techniques. The following discussion is closely related to the treatment of Hoult (*6*) for the rotating-frame NMR imaging method.

To simplify the notation, we discuss the local response from a single volume element located at an arbitrary position **r** and resonance frequency ω. To take into account both the resonance and the spatial frequency distributions, the total response from the sample should include the integrals over a certain spin density $\rho(\omega, \mathbf{r})$ and lineshape function.

In the original 2D spatially resolved NQR spectroscopy technique, the response is acquired following a single RF pulse of variable length applied to the spin system at thermal equilibrium. After the application of the first pulse of length t_1, the NQR signal is recorded in the detection period t and one obtains the previously published result

$$G_{\theta,\phi}(t, t_1) \sim -\lambda(\theta, \phi)\sin \omega_1'(\mathbf{r})t_1 \exp[i(\omega - \Delta\omega)t]. \quad [1]$$

Equation [1] shows that the evolution during the preparation

period t_1 modulates the amplitude of the signal, i.e., the response results proportional to the sine of the effective nutation angle $\omega_1'(\mathbf{r})t_1$.

Amplitude modulation, represented by the sine term in Eq. [1], can be understood as a superposition of two equally weighted signals with the frequencies ω_1' and $-\omega_1'$ during the preparation pulse of length t_1. Therefore, a 2D Fourier transformation of Eq. [1],

$$A_{\theta,\phi}(\omega,\ \omega_1) = \int_{t=0}^{+\infty}\int_{t_1=0}^{T} G_{\theta,\phi}(t,\ t_1)\sin(\omega_1 t_1)e^{-i\omega t}dt_1dt,$$

leads to the spectrum

$$A_{\theta,\phi}(\omega,\ \omega_1) = S(\omega)\lambda(\theta,\ \phi)\left[\frac{\sin(\omega_1' - \omega_1)T}{2(\omega_1' - \omega_1)} - \frac{\sin(\omega_1' + \omega_1)T}{2(\omega_1' + \omega_1)}\right]. \quad [2]$$

It was assumed that truncation effect is important only in the second dimension t_1. The complex function $S(\omega)$ represents the natural NQR lineshape. Because the amplitude-modulated signal is a real function in the second domain, the Fourier spectrum A in Eq. [2] contains pure absorption lineshapes at the frequency coordinates $(\omega_0,\ \omega_1')$ and $(\omega_0,\ -\omega_1')$. Therefore, the two-dimensional spectrum appears in two antisymmetric copies in the second frequency domain at positive and negative nutation frequencies.

For the phase-encoding variant a second homogeneous pulse, 90° out of phase with respect to the first one, is applied. The induced signal results proportional to

$$G_{\theta,\phi}(t,\ t_1,\ t_2,\ \Delta\omega) \sim \lambda(\theta,\ \phi)[i\ \sin\ \omega_2' t_2\ \cos\ \omega_1'(\mathbf{r})t_1 - \sin\ \omega_1'(\mathbf{r})t_1]\exp[i(\omega - \Delta\omega)t]. \quad [3]$$

In the case of a single crystalline sample with only one physical site per unit cell, i.e., with a single orientation θ_1 and ϕ_1, the length of the second pulse can be adjusted so that the condition $\omega_2' t_2 = \pi/2$ is fulfilled over the whole volume of the sample, and the signal becomes

$$G_{\theta_1,\phi_1}(t,\ t_1) \sim i\lambda(\theta_1,\ \phi_1)\exp[i\omega_1'(\mathbf{r})t_1 + i(\omega - \Delta\omega)t]. \quad [4]$$

Comparison with Eq. [1] shows that the evolution in t_1 now modulates the *phase*, with the effective nutation angle $\omega_1'(\mathbf{r})t_1$, rather than the *amplitude* of the nuclear signal.

From Eq. [4], the complex 2D Fourier transform of the phase-modulated signal is

$$P_{\theta_1,\phi_1}(\omega,\ \omega_1) = S(\omega)\lambda(\theta_1,\ \phi_1)\left[\frac{e^{i(\omega_1' - \omega_1)T} - 1}{(\omega_1' - \omega_1)}\right]. \quad [5]$$

The phase modulation of the signal leads to the well-known phase twist problem of two-dimensional Fourier spectrum, which originates in the mixing of absorption and dispersion data components. It is not possible to phase the 2D spectrum and the absolute-value display has much lower resolution than pure absorption lineshapes. Therefore, we use the technique described by Hoult (*6*) to remove the phase twist and to exhibit the 2D spectrum P in Eq. [5] with no dispersive components. We repeat the experiment but change the phase of the second pulse by 180°. After taking the conjugate Fourier transformation of the resulting signal, the spectrum results in

$$P'_{\theta_1,\phi_1}(\omega,\ \omega_1) = S(\omega)\lambda(\theta_1,\ \phi_1)\left[\frac{\exp^{-i(\omega_1' - \omega_1)T} - 1}{(\omega_1' - \omega_1)}\right]. \quad [6]$$

From Eqs. [5] and [6], the spectrum is

$$\frac{P - P'}{2} = iS(\omega)\lambda(\theta_1,\ \phi_1)\frac{\sin(\omega_1' - \omega_1)T}{(\omega_1' - \omega_1)}.$$

The last equation describes a single peak in pure absorption mode in the nutation frequency domain, and shows the $\sqrt{2}$ improvement in sensitivity compared with the spectrum of Eq. [2] obtained with the amplitude-modulated technique.

Application of the Phase-Encoding Technique to Powder Samples

In polycrystalline or powder samples the random distribution of the EFG's orientations must be considered. For a specimen with an isotropic distribution of EFG's orientation all the values of θ and ϕ occur. Therefore, it is no longer possible to apply a uniform 90° pulse for phase encoding to all nuclei in the object. The reconstruction of quadrupole nuclear density in powder or polycrystalline samples has been discussed in previous papers (*14*, *15*). The standar Fourier transform analysis fails to produce accurate profiles and special nonlinear reconstruction algorithms have been developed to take into account the actual point response function with powder samples. Fourier-based deconvolution procedure (*14*) and maximum-entropy method (MEM) (*15*) are not linear algorithms and a comparison of signal-to-noise ratio between amplitude- and phase-modulated technique cannot be made from such spectra. To evaluate the reconstructed profiles, Fourier-transformed and MEM spectra are presented under Experiments and Results for the powder samples. The Fourier transform is a crude reconstruction procedure but it is a linear method and allows us to

draw some conclusions about the resulting signal-to-noise ratios of the encoding techniques.

The powder NQR signal is calculated as

$$G(\omega, \omega_1) = \frac{1}{4\pi} \int_0^{\pi} d\theta \sin\theta \int_0^{2\pi} d\phi G_{\theta,\phi}(\omega, \omega_1), \quad [7]$$

where $G_{\theta,\phi}$ denotes the contribution to the macroscopic signal due to a crystallite at θ and ϕ. From the analysis of Eq. [3] it can be seen that for arbitrary values of θ and ϕ the resulting signal recorded with the two-pulse encoding technique is a mixture of amplitude and phase encoding. Only for those quadrupole nuclei with a particular orientation that satisfies the condition $\omega_2' t_2 = \pi/2$ is a pure phase-modulated nutation spectrum obtained.

Our numerical calculations of the spin density reconstructed from Eqs. [3] and [7] show that the powder distribution in the 90° pulse introduces minor distortions in the profiles. Experimental results also show that despite the orientation dependence of the second pulse the two-pulse sequence is effective to achieve phase encoding (see also Fig. 2 in Ref. (*8*)). The reason is that the efficiency of the 90° plane rotation depends on the function $\lambda(\theta, \phi)$, but the amplitude of the observed magnetization is weighted by the same function. As an example we can analyze the case of $\eta = 0$, then $\lambda = \sqrt{3} \sin\theta/2$. The length of the nominal 90° pulse for powder corresponds approximately to the first maximum of the Bessel function J_1, then

$$\frac{\sqrt{3}}{2} \gamma B_2 t_2 = \pi/\sqrt{3}.$$

Therefore, only those crystals oriented at an angle θ_0 that satisfies $\sin\theta_0 = \sqrt{3}/2$ experience a perfect phase modulation. When the orientation θ deviates from this condition, the signal results modulated in both amplitude and phase. When θ goes to zero, the mixture between amplitude and phase modulation increases but then the signal intensity approaches zero.

It should be mentioned that a similar problem is faced with the implementation of phase-modulated rotating-frame imaging (PMRFI) in NMR using a transmitter surface coil (*16*). It has been demonstrated that despite the presence of large B_1 inhomogeneities to apply uniform 90° plane rotations throughout the sensitive volume of the coil, the PMRFI technique provides accurate localization and the expected $\sqrt{2}$ improvement in sensitivity compared to the amplitude-modulated version. It was later demonstrated that adiabatic plane-rotation pulses with a higher degree of tolerance to B_1 nonuniformities can be implemented to execute uniform 90° pulses using a single-surface coil for transmission and detection (*17*).

In our implementation of the PMRFI NQR experiments the nonuniform 90° pulse is not due to spatial field inhomogeneities but to the random orientation of crystals in the powder samples. It might be possible to use adiabatic plane-rotation pulses to improve the efficiency of phase encoding, but its implementation is not discussed in this work.

RAPID PHASE-ENCODED ROTATING-FRAME TECHNIQUE

The rapid rotating-frame method (*4*) is based on the application of the pulse train

$$[(G_1 \Delta t_1)_0 - \tau -]_n,$$

with τ much shorter than the transverse-relaxation time. For on-resonance spins, or those with a frequency offset that satisfies $\Delta\nu\tau k$, with k an integer, the flip angles induced by G_1 accumulate and the amplitude of the signal acquired in the nth acquisition interval is modulated with the effective flip angle $\alpha_1 \gamma \lambda(\theta, \phi) B_1 n \Delta t_1$. In absence of dephasing during the short acquisition window τ, the one-shot technique yields the same amplitude-modulated signal, or pseudo-FID, as the 2D method (*4*).

To convert this technique to a phase-modulated variant we insert a $(B_2 t_2)_{\pi/2}$ pulse prior to acquisition. After the short interval of free evolution τ, a $(B_2 t_2)_{-\pi/2}$ pulse put the magnetization back onto the original nutation plane of the rotating frame. Then, the spatially dependent nutation angle advances with the next gradient pulse. The pulse sequence for rapid phase-modulated rotating-frame method results in

$$[(G_1 \Delta t_1)_0 (B_2 t_2)_{\pi/2} - \tau - (B_2 t_2)_{-\pi/2}]_n.$$

Using the QIR formalism it is straightforward to demonstrate, in the absence of spin interactions, the equivalence of the nutation signals obtained by both the 2D and the 1D phase-encoding techniques.

EXPERIMENTS AND RESULTS

To produce both homogeneous and inhomogeneous RF fields, the double-coil arrangement described in Ref. (*1*) was implemented. The RF gradient is produced with the aid of an anti-Helmholtz coil of 20 mm in diameter. A solenoid, 18 mm in diameter and 30 mm long, coaxial to the anti-Helmholtz, is used as the second transmitter/receiver coil. A major advantage of this coil arrangement is that the coils are decoupled per se thus avoiding the use of active decoupling circuits. The RF fields are parallel as required for the phase-encoding technique. This is also a suitable coil configuration to test the discrimination of positive and negative coordinates defined by a zero-crossing B_1 gradient. The coils were tuned at 34,260 MHz, the ^{35}Cl-resonance of paradichlorobenzene at room temperature.

A Kalmus LP 1000 power amplifier drives the anti-Helm-

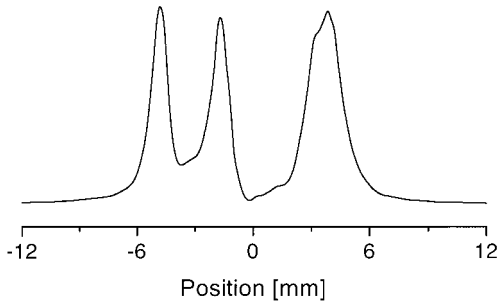

FIG. 1. One-dimensional spatial distribution reconstructed by the MEM procedure from data obtained with the 2D phase-encoding technique. The profile represents the projection of the three-compartment test object containing paradichlorobenzene in powder: The peaks on the negative axis correspond to the two disks of 2-mm thickness separated by a 2-mm spacer, and the peak on the positive coordinate represents the third 3-mm-thick layer separated from the others by a 3-mm spacer. The actual structure and position of the sample can be reproduced because the profile reconstructed from the phase modulation of the FID signals contains components at the true spatial frequency of the spins.

holtz coil, whereas a 600-W solid-state amplifier (two 300-W Motorola Mod. 827 power amplifiers working in parallel) is used for the solenoidal coil. A phase shifter inserted in one of the two transmitter paths allows us to adjust carefully the relative phase of both channels. A homebuilt RF power switch was implemented to drive each power amplifier independently.

To demonstrate the two-dimensional phase-encoding method for spatial localization in powder materials, we applied the technique in a simple one-dimensional imaging experiment. For the two-dimensional encoding experiments, the NQR sample has three compartments, 10 mm in diameter, containing paradichlorobenzene in powder. Two compartments were 2 mm in depth and were placed in one half of the anti-Helmholtz coil, while the third 3-mm-thick compartment was positioned in the other half. A set of 64 NQR signals was acquired in quadrature as a function of the pulse length starting at 8 μs, incremental steps of 8 μs, and with 10 transients per pulse length. The duration of the nominal 90° pulse, obtained by maximizing the FID excited with a single B_2 pulse, was 20 μs. To keep the image reconstruction procedure simple, the object was positioned in the approximately constant G_1 region of the coil arrangement. Figure 1 shows the profile of the quadrupole nuclear density of the object reconstructed by MEM (*15*) under the assumption of linear B_1 and constant B_2 fields. It is apparent in Fig. 1 that the technique resolves the negative and positive coordinates defined by G_1. Therefore, the resulting spatial distribution shows the actual position of the quadrupole nuclei without quadrature image in the B_1 dimension.

For the rapid rotating-frame experiment, the phantom consists of only two compartments of 10 mm in diameter and 2 mm in depth and was placed in one half of the anti-Helmholtz coil. The train for the rapid phase encoding was composed of inhomogeneous pulses of 10 μs and the length of the 90° pulse was 20 μs, with detection intervals of 40 μs.

Figure 2 shows the spatial profiles resulting from a one-dimensional Fourier transform of an amplitude-modulated (a) and phase-encoding (b) rotating-frame experiments carried out on the two-compartment phantom. Notice the broadening of the peaks representing the quadrupole nuclear distribution in the Fourier-transformed spectra resulting from the powder distribution of nutation frequencies, which is removed using the MEM procedure. Comparison of peak intensities in the Fourier spectra leads us to the conclusion that the PMRFI experiment yields approximately a $\sqrt{2}$ gain in the signal-to-noise ratio compared with the amplitude-modulated technique.

Application of the maximum-entropy reconstruction procedure to a complex pseudo-FID gathered with the rapid phase-modulated technique leads to the profile shown in Fig. 3. As with the 2D technique, the spectrum does not contain the quadrature image of the spatial distribution, because the modulation due to positive and negative values of B_1 produced by the gradient coil can be distinguished by the phase-modulated technique, like quadrature detection in the second frequency

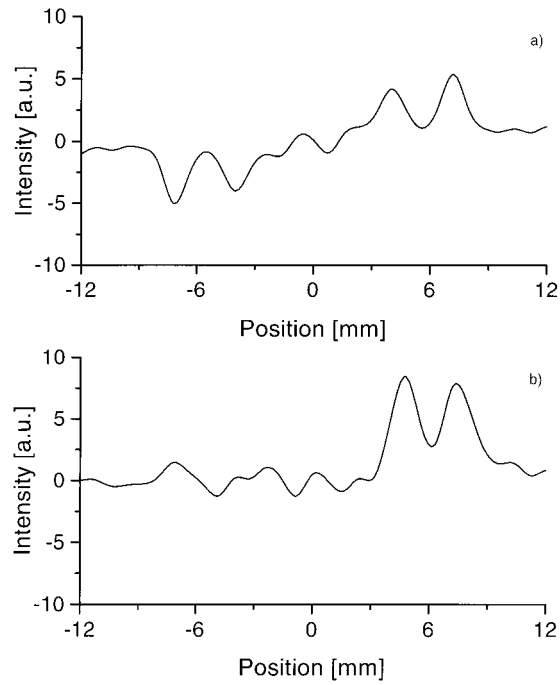

FIG. 2. Fourier reconstructed profiles at the on-resonance frequency from the data set acquired by the rapid 1D amplitude-modulated and phase-encoding experiments. The test object has two compartments; dimensions of each compartment are 2 mm in depth and 10 mm in diameter, separated by a 2-mm-thick spacer. The phantom was located in one half of the anti-Helmholtz coil so that it experiences a single B_1 gradient. The data set (a) was gathered using the amplitude-modulated technique, which shows a quadrature image in the nutation frequency dimension, and spectrum (b) results from the phase-modulated experiment, which shows the gain in signal-to-noise compared with profile (a). Broadening of the peaks results from the powder distribution of the nutation frequencies.

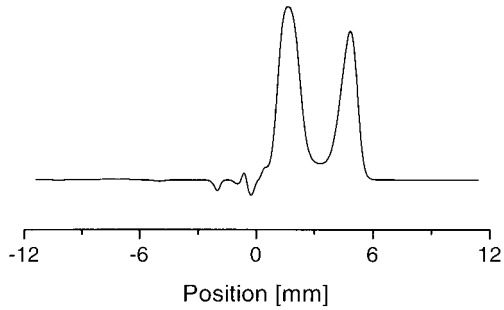

FIG. 3. Spatial profile reconstructed by the MEM procedure from a complex pseudo-FID recorded with the rapid phase-modulated technique. The experiment was carried out on the same two-compartment object that yields the spectra of Fig. 2. The profile appears on one side of the spatial coordinate axis because the sample experience of a single B_1 gradient and the technique enables one to resolve the actual spatial frequencies.

domain. Similar spatial resolution was achieved with the rapid and two-dimensional phase-encoding pulse sequences.

CONCLUSIONS

The experiments reported here demonstrate the feasibility of the phase-modulated spatially resolved spectroscopy and imaging NQR methods in powder samples. Despite the orientation dependence of the encoding radio frequency fields and the lack of uniform plane-rotation pulses, phase-modulation of the NQR signal can be induced by the simple two-pulse sequence and applied for spatial encoding. Our implementation of the technique requires a two-coil arrangement but, in contrast to NMR, the 90° phase-shifted pulses cannot be implemented using perpendicular coils. This is because, in NQR experiments, out-of-phase pulses in the rotating frame are not equivalent to perpendicular RF fields in the laboratory frame. Fourier analysis of the rotating-frame experiments shows that a sensitivity gain is achieved with the phase-modulated technique. Another advantage of the phase-encoding techniques is that they allow one to distinguish the sign of the spatial coordinate which might be advantageous in some experiments.

Besides the applications reported here of the rapid phase-modulated rotating-frame method to NQR, the technique can directly be applied to NMR systems to increase the sensitivity in small-scale high-resolution imaging experiments (*18, 19*).

ACKNOWLEDGMENTS

We thank the National and Provincial Research Councils (CONICET and CONICOR, respectively) for financial support. F.C. thanks CONICET for Research Fellowship. H.R. held a fellowship from CONICET during the course of this work.

REFERENCES

1. E. Rommel, P. Nickel, R. Kimmich, and D. Pusiol, *J. Magn. Reson.* **91,** 630 (1991).
2. E. Rommel, D. Pusiol, P. Nickel, and R. Kimmich, *Meas. Sci. Technol.* **2,** 866 (1991).
3. P. Nickel, H. Robert, R. Kimmich, and D. Pusiol, *J. Magn. Reson. A* **111,** 191 (1994).
4. H. Robert, A. Minuzzi, and D. Pusiol, *J. Magn. Reson. A* **118,** 189 (1996).
5. H. Robert and D. Pusiol, *J. Magn. Reson.* **127,** 109 (1997).
6. D. I. Hoult, *J. Magn. Reson.* **33,** 183 (1979).
7. M. Bloom, E. L. Hahn, and B. Hertzog, *Phys. Rev.* **97,** 1699 (1955).
8. F. Vaca Chavez, F. Casanova, H. Robert, and D. Pusiol, *J. Chem. Phys.* **108** (5), 1881 (1998).
9. J. C. Pratt, *Mol. Phys.* **34,** 539 (1977).
10. A. Vega, *Isr. J. Chem.* **32,** 195 (1992).
11. A. K. Dubey, A. Ramamoorthy, and P. Raghunathan, *Chem. Phys. Lett.* **168,** 401 (1990).
12. Sunyu Su and R. L. Armstrong, *J. Magn. Reson. A* **101,** 265 (1993).
13. A. Ramamoorthy, N. Chandrakumar, A. K. Dubey, and P. T. Narasimhan, *J. Magn. Reson. A* **102,** 274 (1993).
14. E. Rommel, R. Kimmich, H. Robert, and D. Pusiol, *Meas. Sci. Technol.* **3,** 446 (1992).
15. H. Robert, D. Pusiol, E. Rommel, and R. Kimmich, *Z. Naturforsch.* **49a,** 35 (1994).
16. M. J. Blackledge, B. Rajagopalan, R. D. Oberhaensli, N. M. Bolas, P. Styles, and G. K. Radda, *Proc. Natl. Acad. Sci. USA* **84,** 4283 (1987).
17. K. Hendrich, H. Merkle, S. Weisdorf, W. Vine, M. Garwood, and K. Ugurbil, *J. Magn. Reson.* **92,** 258 (1991).
18. P. Maffei, P. Mutzenhardt, A. Retournard, B. Diter, R. Raulet, J. Brondeau, and D. Canet, *J. Magn. Reson. A* **107,** 40 (1994).
19. F. Humbert, B. Diter, and D. Canet, *J. Magn. Reson. A* **123,** 242 (1996).